Available online at www.sciencedirect.com
SCIENCE DIRECT
Journal of Catalysis 235 (2005) 327–332
JOURNAL OF CATALYSIS
www.elsevier.com/locate/jcat

Catalytic oxidation of CO by aqueous polyoxometalates on carbon-supported gold nanoparticles

Won Bae Kim [a,1], G.J. Rodriguez-Rivera [a], S.T. Evans [a], T. Voitl [a], J.J. Einspahr [b], P.M. Voyles [b], J.A. Dumesic [a,*]

[a] *Department of Chemical and Biological Engineering, University of Wisconsin, 2014 Engineering Hall, 1415 Engineering Drive, Madison, WI 53706, USA*
[b] *Department of Materials Science and Engineering, University of Wisconsin, 1509 University Avenue, Madison, WI 53706, USA*

Received 18 March 2005; revised 2 June 2005; accepted 6 June 2005

Available online 28 September 2005

Abstract

Oxidation of CO was carried out at room temperature with the use of aqueous solutions of polyoxometalates over carbon-supported gold catalysts. The turnover frequency (TOF) for CO oxidation reaches high rates of 4.7 s^{-1} for catalysts with average gold particle sizes of 5 nm, estimated by X-ray diffraction (XRD) and transmission electron microscopy (TEM), and with gold loading of 1 wt%, determined by elemental analysis. Lower rates are observed at higher gold loadings, which may be attributed to mass transport limitations in the present system and to the presence of larger gold particles. Carbon-supported gold catalysts exhibit selective oxidation of CO versus H_2, and a small increase in the selectivity for CO versus H_2 oxidation is observed as the gold particle size decreases from 12.1 to 5.6 nm.
© 2005 Elsevier Inc. All rights reserved.

Keywords: CO oxidation; Gold catalysts; Nanoparticles; Polyoxometalates; Hydrogen; Fuel cells

1. Introduction

Following the initial discovery by Haruta et al. [1,2] that nanoparticles of gold on oxide supports show high activity for oxidation of CO with O_2 at room temperature, extensive research has been conducted in heterogeneous catalysis to understand and take advantage of the unique properties of these materials (e.g., [3–5]). The low-temperature catalytic properties of gold catalysts are of particular relevance for the production of fuel-cell-grade H_2, since the inevitable presence of CO in H_2-rich gas streams produced from catalytic reforming of hydrocarbons [6] strongly poisons Pt-based anodes in H_2 fuel cells [7].

We have recently reported a new process that directly utilizes CO as a source of energy by converting it with water to CO_2 via an aqueous solution containing a reducible polyoxometalate (POM) compound, $H_3PMo_{12}O_{40}$, over gold catalysts [8]. As represented in the following overall reaction based on a two-electron transfer (i.e., oxidation of one CO molecule), the POM serves as an oxidizing agent for CO and as an energy storage agent for electrons produced from the reaction of dissolved CO, denoted as $CO_{(s)}$ and liquid water:

$$CO_{(s)} + H_2O_{(l)} + 2PMo_{12}O_{40}{}^{3-}{}_{(aq)} \rightarrow CO_{2(g)} + 2H^+{}_{(aq)} + 2PMo_{12}O_{40}{}^{4-}{}_{(aq)}.$$

A possible reaction scheme for room-temperature CO oxidation with liquid water assisted by the aqueous POMs was proposed in an earlier work [9]. The proposed mechanism assumes a heterolytic process to form protons that are solvated by liquid water molecules [10], as represented below. An electron is subsequently transferred from the gold catalyst to the POM. The subscript s denotes a dissolved species in the aqueous solution, the asterisk * denotes a surface

* Corresponding author. Fax: +1 608 262 5434.
E-mail address: dumesic@engr.wisc.edu (J.A. Dumesic).
[1] Current address: Department of Materials Science and Engineering, Gwangju Institute of Science and Technology (GIST), Oryong-dong 1, Buk-gu, Gwangju 500-712, South Korea.

0021-9517/$ – see front matter © 2005 Elsevier Inc. All rights reserved.
doi:10.1016/j.jcat.2005.06.003

site of gold, and $e^-(POM)_{(aq)}$ indicates a POM reduced by 1 electron.

$$CO_{(s)} + * \rightarrow CO*,$$

$$H_2O_{(l)} + * + (POM)_{(aq)} \rightarrow OH* + H^+_{(aq)} + e^-(POM)_{(aq)},$$

$$CO* + OH* \rightarrow COOH* + *,$$

$$COOH* + (POM)_{(aq)} \rightarrow CO_{2(g)} + H^+_{(aq)} + e^-(POM)_{(aq)} + *,$$

Net:

$$CO_{(s)} + H_2O_{(l)} + 2(POM)_{(aq)} \rightarrow CO_{2(g)} + 2H^+_{(aq)} + 2e^-(POM)_{(aq)}.$$

To utilize these protons and electrons produced from water, we demonstrated that the resulting aqueous solutions containing electrons associated with the reduced POM and protons produced from water during CO oxidation to CO_2 could be delivered to a carbon anode of a proton exchange membrane (PEM) fuel cell, leading to the production of electrical energy upon re-oxidation of the reduced POM to its initial oxidized state [8]. It was also demonstrated [9] that this room-temperature process could be used to selectively remove CO in H_2-rich gas streams over carbon-supported gold catalysts (e.g., selective oxidation of CO in a gas stream containing 0.1% CO in H_2).

In this note, we report results from an investigation of the effects of gold particle size for the oxidation of CO by liquid water with POM (i.e., aqueous POM solutions) over carbon-supported gold catalysts. A series of carbon-supported gold catalysts (Au/C) were prepared with a systematic variation of the gold loadings from 0.1 to 20 wt% and with a change of gold particle sizes from 5.6 to 12.1 nm at a fixed loading of gold (1 wt% Au/C), as estimated by X-ray diffraction (XRD) and transmission electron microscopy (TEM). We have used carbon as a support for gold nanoparticles to avoid possible complexities caused by participation of oxide supports in the reaction scheme, such as the involvement of OH [3] or activated O species [11] from the support as oxidizing agents for CO. In fact, whereas most studies of CO oxidation by O_2 involve the use of gold nanoparticles on various oxide supports, we find that CO oxidation by aqueous POM compounds takes place at high rates on carbon-supported gold nanoparticles, perhaps because the catalyst does not need to dissociate O_2 under our reaction conditions.

2. Experimental

2.1. Preparation of Au/C catalysts

Carbon-supported gold catalysts were made from surfactant-protected gold particles in aqueous solution [12]. The primary carbon support used in this study was Vulcan XC72 (Cabot Corp.), which was first acid-pretreated by suspension in a 6 M aqueous HCl solution with vigorous stirring for 12 h. The carbon was then washed several times with Millipore de-ionized water until the solution pH was around 6, followed by filtration and drying for 5 h in air at 393 K. The surfactant *N*-dodecyl-*N*,*N*-dimethyl-3-amino-1-propan sulfonate (SB, purchased from Aldrich) was used to stabilize gold sols in aqueous solution. With this method, different gold loadings on the carbon were synthesized from 0.1 to 20 wt%. Typically, for the preparation of a 1 wt% Au/C catalyst, 1.27 cm^3 of 0.01 M aqueous SB solution was added to an auric solution containing 0.1 g of 10 wt% $HAuCl_4 \cdot 3H_2O$ in 173 cm^3 of water (i.e., molar ratio of SB/Au = 1:2) under vigorous stirring. Aqueous Na_2CO_3 was added with stirring until the solution pH reached around 8. A freshly prepared aqueous $NaBH_4$ solution (5 cm^3 of 0.05 M) was added dropwise over 4 h with a syringe pump (Harvard Apparatus, Inc.), corresponding to a 10:1 molar ratio of $NaBH_4$:Au. A few minutes after formation of a gold sol, as indicated by a color change of the solution to a ruby red color, 1 g of the pretreated carbon was added to the gold sol with vigorous stirring. The resulting slurry was filtered for 2 h after all of the $NaBH_4$ was added. The catalyst was then washed thoroughly with water and dried for approximately 40 h in a vacuum chamber to remove absorbed water. We used this catalyst without heat treatment for reaction kinetic studies. The water content of each catalyst was measured by monitoring of the weight of a catalyst aliquot during heat treatment (393 K for 4 h), showing that the Au/C catalysts contained 5–10% water by weight.

As a reference for comparison with the properties of the Au/C catalysts prepared in this study, we also studied the catalytic properties of the "Type D" Au/C catalyst supplied by the World Gold Council (WGC, Lot #4D, London SW1Y 5JG, United Kingdom), containing 0.8 wt% Au as determined by atomic absorption/inductively coupled plasma (ICP) emission. The average Au particle diameter measured by TEM was 10.5 nm, and the Au particle diameter estimated by powder X-ray diffraction (XRD) was 8.0 nm.

2.2. Reaction kinetics measurements

In a typical experiment, a batch reactor was loaded with 20 cm^3 of 0.05 M POM solution, and the Au/C catalyst was purged three times with N_2 or He and then filled to a pressure of 14.8 bar with pure CO or a CO:H_2 mixture (0.1–1% CO in H_2), supplied by Linde Gas Group (Independence, OH, USA). The reactor was a stainless-steel vessel (approximately 350 cm^3 volume), in which the POM solution and catalyst were placed in a glass liner with a magnetic stirrer. We analyzed gas-phase products at specific times by releasing pressure from the batch reactor to an online gas chromatograph (GC, Hewlett Packard 5890) equipped with a thermal conductivity detector and a 30-foot Alltech column packed with 120/100-mesh Hayesep DB that used helium as a carrier. The column was initially kept at 313 K for 10 min, and the temperature was then ramped at 20 K min^{-1} to 513 K, where it was kept for 10 min. The temperature

program allowed the analysis of noncondensable gases and water vapor. We have used several gas mixtures for reaction kinetics studies and for GC calibrations. These mixtures included 1 and 0.1% CO in H_2 balance, UHP (99.999%) H_2, UHP (99.995%) CO, and 1.01% CO_2 in N_2 balance (formulated by Linde Gas Group, Independence, OH, USA). We measured the rate of H_2 oxidation by monitoring the color change in the POM solution with a UV/vis spectrometer operating at 500 nm [9].

The 1:1 stoichiometry between CO consumed and CO_2 produced was corroborated by analysis of the gas products with the GC for repeated experiments, and the ratio of the amount of CO_2 produced to the amount of CO consumed was 1.0 ± 0.1. The electron balance determined from the extent of POM reduction and the amount of CO_2 produced agreed within 20% for the following overall reaction:

$$\mathrm{CO} + \mathrm{H_2O} + 2(\mathrm{POM})_{(aq)} \rightarrow \mathrm{CO_2} + 2\mathrm{H^+} + 2\mathrm{e^-}(\mathrm{POM})_{(aq)}.$$

In this calculation, the total number of electrons produced and subsequently stored in the POM solution was calculated by integration of the electrical current versus time and division by the Faraday constant while the reduced POM was completely re-oxidized in an anode of an electrochemical cell [8] for the following reaction:

$$2\mathrm{H^+} + 2\mathrm{e^-}(\mathrm{POM})_{(aq)} + (1/2)\mathrm{O_2} \rightarrow \mathrm{H_2O} + 2(\mathrm{POM})_{(aq)}.$$

2.3. Characterization of catalysts

X-ray diffraction patterns were collected for various Au/C catalysts to estimate the gold particle sizes, with the use of a model XRG3000 diffractometer operating with a Cu-K_{α_1} ($\lambda = 1.5405$ Å) source and a CPS120 curved detector with 3915 active channels (INEL Inc.). The source was operated at 40 kV and 30 mA.

The morphology and size distribution of gold particles were studied with a Philips CM200 Ultra Twin high-resolution TEM operating at 200 kV with a 1.9-Å point resolution. All TEM images on the Au/C samples were obtained in the absence of an objective aperture. We prepared the samples for TEM imaging by depositing a suspension containing the Au/C particles on carbon-coated TEM grids and allowing the water to evaporate, leaving the particles suspended on the carbon support.

Gold loadings on all catalysts were determined by inductively coupled plasma (ICP) analysis, showing that the nominal gold loadings (in wt% on carbon) were the same as their actual loadings within ±5%, as presented in Table 1.

3. Results and discussion

Physical properties of the gold catalysts prepared in this study are presented in Table 1. The average diameters of gold particles estimated by XRD were generally smaller by about 2.5 nm for each sample compared with those measured by TEM in our measurement conditions. We varied the gold loading on these catalysts from 0.1 to 20 wt% by changing the concentration of the gold precursor during the synthesis procedure. The rates of CO oxidation versus gold loading of these catalysts are plotted in Fig. 1, wherein the rates are defined as (1) the specific rate of CO oxidation based on the catalyst weight ($\mu mol_{CO_2}\, g_{cat}^{-1}\, min^{-1}$) and (2) the turnover frequency (TOF, in s^{-1}), in which the rate is normalized by the number of surface sites estimated from the average particle diameter determined by XRD and TEM. We have calculated the dispersion of the gold particles, using the atomic density of (111) planes, via the following equation:

$$D\ (\text{dispersion}) = 1.41/d_p,$$

where d_p is the particle diameter in nanometers. All rates were measured at initial conversions of POM of less than 10%, corresponding to less than one electron per POM unit. (The highest reduction of POM under our reaction conditions corresponds to five electrons transferred to each POM unit [8].) The POM used in this work has the Keggin structure [13] with multiple redox steps via single and multi-electron transfer processes [14].

The specific rate increases with gold loading from 0.1 to 4 wt%, and it decreases monotonically with further increases in the gold loading above 4 wt%. This behavior could be related to an increase in the gold particle size at higher loadings of gold on carbon; that is, the gold particles are substantially larger and have agglomerated at gold loadings from 10 to 20 wt%. The results from XRD show that the gold particles have diameters from 9 to 11 nm for gold loadings from 10 to 20 wt%, whereas the gold particles are smaller (5–6 nm) for gold loadings from 0.5 to 4 wt%. This trend is also observed in the average particle diameters determined from TEM images, as shown in the representative micrographs in Fig. 2. The specific rate of the reference catalyst

Table 1
Physical properties of Au/C catalysts with different Au loadings

Au loading (wt%) from ICP[a]	Average particle size of Au (nm)	
	From XRD[b]	From TEM[c]
0.10	7.2	11.9 ± 2.0
0.49	5.2	
0.81	5.6	7.9 ± 2.2
1.0	5.0	
2.0	5.0	
3.9	4.7	6.8 ± 1.7
9.2	8.7	
20.1	10.4	
10.0[d]	4.5	7.5 ± 2.4
0.8[e]	8.0	10.5 ± 3.0

[a] Inductively coupled plasma (ICP) analysis (±5% in the determined wt%).
[b] Mean diameter of gold estimated by line broadening of powder XRD peak at $2\theta = 38.2°$ using the Scherrer equation (±1 nm).
[c] Mean diameter of gold from TEM images using at least 100 particles.
[d] 10 wt% Au/C catalyst prepared using a diluted gold solution compared to the normal 10 wt% catalyst with an actual loading of 9.2 wt% by ICP.
[e] Au/C catalyst supplied from the World Gold Council.

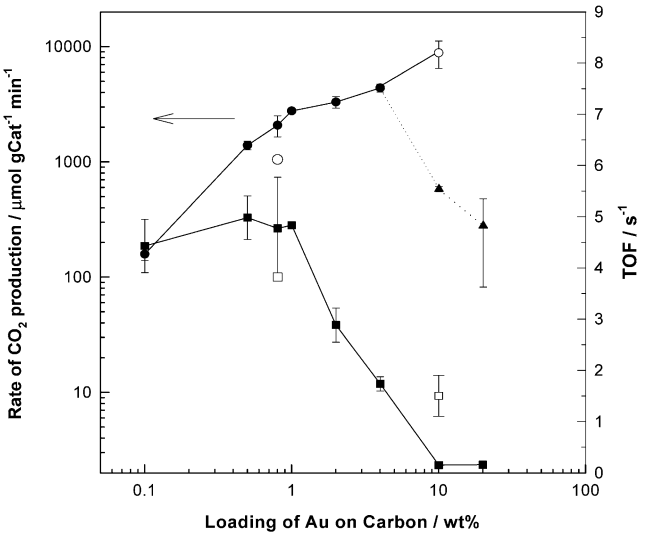

Fig. 1. Rates of CO oxidation over Au/C catalysts with different gold loadings. Reaction rates were measured at initial conversions of POM less than 10%. Values of TOF were estimated from dispersion of gold measured by XRD and TEM. Legend: Rates per gram of catalyst (●) and TOF (■); rates per gram of catalyst (▲) of poorly dispersed 10 and 20 wt% Au/C catalysts; rates per gram of catalyst (○) and TOF (□) at 0.8 wt% for WGC; rates per gram of catalyst (○) and TOF (□) at 10 wt% for Au/C prepared from diluted gold sols.

from the WGC is also shown as an open symbol at 0.8 wt% in Fig. 1. In addition, we have also measured the rate over a 10 wt% Au/C catalyst that was prepared with the use of a diluted gold sol (with the same gold concentration in aqueous solution as the 1 wt% Au/C catalyst), and this result is also presented as an open symbol in Fig. 1. This 10 wt% catalyst had smaller gold particles compared with the 10 wt% catalyst prepared by the standard method (compare Figs. 2e and 2f). The 10 wt% Au/C made with the diluted gold solution (open symbols at 10 wt% Au) shows higher activity than the normal 10 wt% Au catalyst, because of the smaller gold particles in this former sample. The gold particles for this catalyst are similar in size to the catalysts with lower loadings, and the plot of rate per gram of catalyst in Fig. 1 does not show a decrease at higher loadings when this 10% Au/C catalyst is considered.

When the specific rates are normalized by the number of surface sites, as estimated from the TEM images, the TOFs for gold loadings from 0.1 to 1 wt%, including the WGC catalyst, are similar within experimental error, as seen in Fig. 1. In contrast, the TOF decreases at gold loadings of 2 wt% or higher, as seen in Fig. 1. XRD and TEM measurements indicate that the average particle sizes of the 2 and 4 wt% catalysts are similar to those with lower gold loadings. Therefore, the decrease in TOF at these catalysts is probably caused by mass transport limitations. This behavior is also seen for the 10 wt% Au/C sample prepared with the diluted sol, because this catalyst has a low TOF, despite having gold particles as small as those present on samples with gold loadings near 1 wt% (see the TEM images of Fig. 2f). Also, as noted above, the rate of CO oxidation per gram of

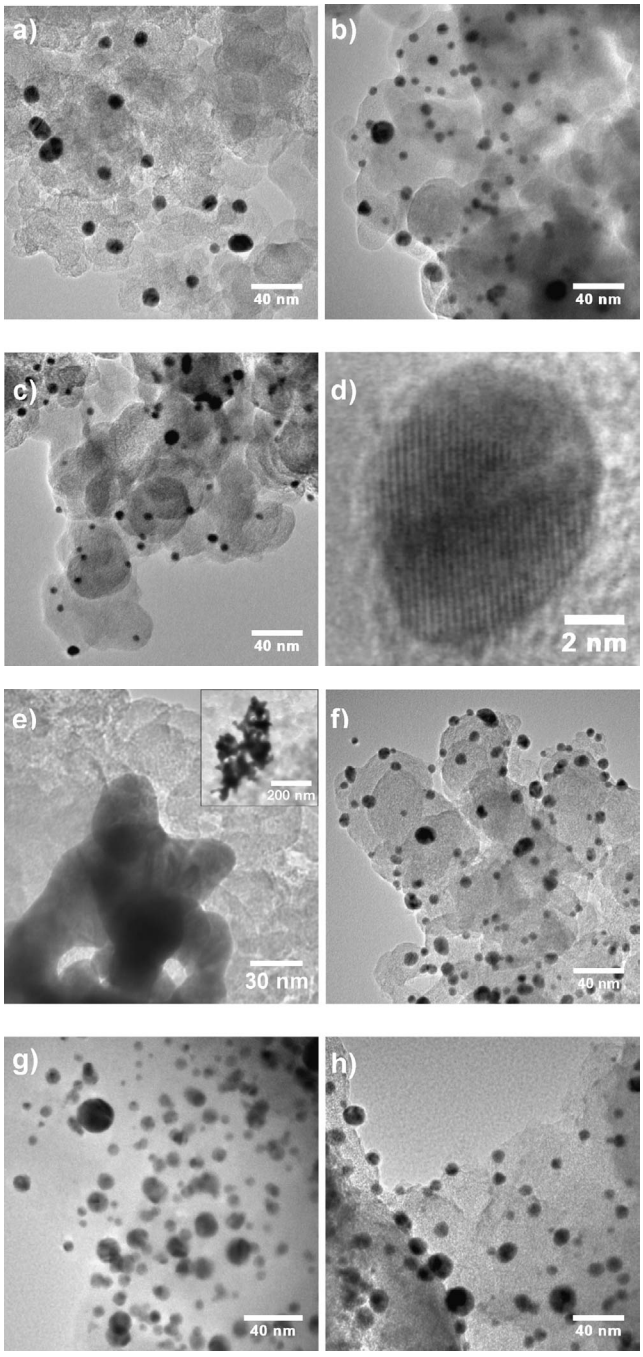

Fig. 2. TEM images of Au/C catalysts with different loadings. (a) 0.1 wt%, (b) 0.8 wt%, (c) 4 wt%, (d) high resolution image showing lattice fringes of a gold nanoparticle from the 4 wt% Au/C catalyst. The scale bar is 40 nm for (a)–(c) and 2 nm for (d). (e) 10 wt%, (f) 10 wt% with a 10 times more diluted gold sol, (g) the fresh Au/C catalyst from WGC, (h) the spent Au/C catalyst from WGC. The scale bar is 30 nm for (e) and 40 nm for (f)–(h).

catalyst becomes nearly constant at the higher gold loadings when the 10 wt% Au/C sample prepared with the diluted sol is considered. The normal Au/C samples with the higher gold loadings of 10 and 20 wt% show very low rates, which can be ascribed to the very large sizes of the primary gold particles, as determined by XRD. Furthermore, the low rates

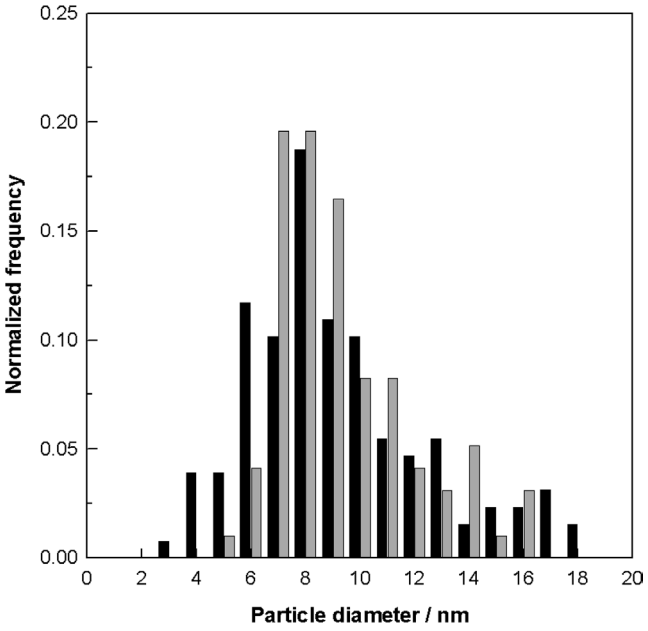

Fig. 3. Gold particle size distribution measured by TEM for the fresh WGC Au/C catalyst (black bar) and the spent WGC Au/C catalyst (gray bar) after oxidation of CO with the aqueous POM solution. Legend: fresh Au/C from the World Gold Council (black bar); spent Au/C from the World Gold Council (gray bar).

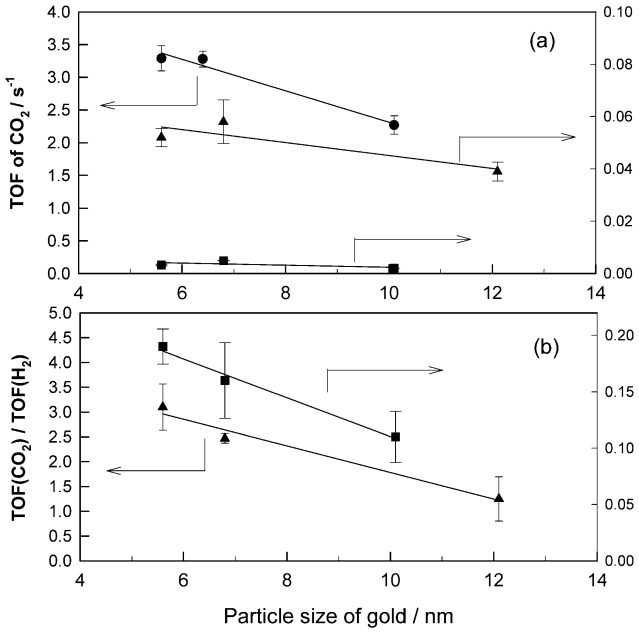

Fig. 4. Rates of CO oxidation over 1 wt% Au/C catalysts with different gold particle sizes estimated by XRD. (a) TOF for CO oxidation with 14.8 bar of 99.995% CO gas (●), with 14.8 bar of gas mixtures of 1% CO in 99% H_2 (▲), and 0.1% CO in 99.9% H_2 (■), (b) the rate ratios of CO oxidation to H_2 oxidation with the same symbol denotation as (a).

for these two samples may also be related to the additional mass transfer limitations caused by agglomeration of these large particles, as shown in the TEM images.

Fig. 3 shows the particle size distribution of gold measured by TEM for the fresh WGC catalyst and the spent catalyst after reaction kinetics measurements of CO oxidation in aqueous POM solutions. The particle size distribution appears to be slightly narrower after reaction, showing more particles with diameters of 7–10 nm for the spent catalyst compared with the fresh catalyst, which shows more particles with diameters of 3–6 nm together with a few very large particles (40–80 nm) that are not included in the figure. We have observed that the specific rate of CO oxidation on the WGC catalyst decreases initially by about 20% in aqueous POM solution, followed by much slower deactivation thereafter, such that about 50% of the initial catalytic activity is retained after exposure to 0.05 M POM for 3 months [9]. This initial decrease in the rate of CO oxidation is consistent with the observed growth noted in Fig. 3 of the smaller particles to sizes of 7–10 nm.

Fig. 4 shows rates of CO oxidation with pure CO and with 0.1 or 1% CO in H_2 gas mixture (i.e., preferential oxidation of CO in H_2) as a function of the gold particle size estimated by XRD. A Au/C (on Black Pearl 2000 carbon support) catalyst with a gold loading of 1 wt% was heat-treated in air at temperatures from 573 to 673 K for 2 h to increase the average particle size of gold from 5.6 to 6.4 nm and from 5.6 to 12.1 nm, respectively. Note that in this range of particle sizes, the surface morphology with respect to surface sites with different coordination numbers should change moderately, whereas more dramatic change in the surface coordination would take place for particles less than 4 nm in size, and no significant changes would be expected for the particle diameter exceeding 10 nm. As seen in Fig. 4a, a modest improvement in the TOF for oxidation of pure CO appears to be caused by a decrease in the gold particle size from 10.1 to 5.6 nm, suggesting that surface sites with low coordination numbers may be more active. For the preferential oxidation of CO, it seems that the TOF for the oxidation of CO in the presence of H_2 also increases modestly with decreasing gold particle size under our reaction conditions, that is, for rates with CO concentrations of 0.1 and 1% in H_2. It is interesting to note that the ratio of the rate of CO oxidation to the rate of H_2 oxidation also appears to be a function of the gold particle size (see Fig. 4b), such that smaller gold particles appear to be more selective for the preferential oxidation of CO in the presence of H_2. This effect leads to an enhancement of the rate ratio by a factor of 2–3 when the gold particle size decreases from 12.1 to 5.6 nm. We note that whereas Au/C catalysts show high selectivity for CO versus H_2 oxidation, other carbon-supported metals (e.g., Pt, Pd, and Ir) exhibit high rates of H_2 oxidation [9]. This high selectivity of gold for CO versus H_2 oxidation may be related to fact that the energetics for the dissociative adsorption of H_2 on gold are far less favorable compared with those of other transition metals [15,16].

We have shown in this research note that high rates of CO oxidation by liquid water with polyoxometalates can be achieved over carbon-supported gold catalysts containing gold particles with sizes from 5 to 8 nm at gold loadings up

to about 1 wt%. The rate of CO oxidation becomes subject to mass transport limitations at gold loadings from 2 to 4 wt% for the present reaction conditions. The TOFs for CO oxidation by liquid water with polyoxometalates reach values of about 5 s^{-1} for gold loadings from 0.1 to 1 wt% in pure CO gas. In addition, good performance can be achieved for the selective oxidation of CO in H_2-rich gas mixtures, suggesting that this catalytic system shows promise for effective removal of CO from H_2-rich gas streams at room temperature. The TOF for CO oxidation increases modestly as the size of the gold particles decreases from 12.1 to 5.6 nm, and the smaller particles also show better selectivity for the oxidation of CO in the presence of H_2.

Acknowledgments

This work was supported by the U.S. Department of Energy, the National Science Foundation, and Daimler-Chrysler. Fellowships were provided by the Camille and Henry Dreyfus Foundation and the Graduate Engineering Scholars program. We thank the World Gold Council for providing gold catalysts and the Materials Science & Engineering Department of University of Wisconsin for providing facilities.

References

[1] M. Haruta, T. Kobayashi, H. Sano, N. Yamada, Chem. Lett. 2 (1987) 405.
[2] M. Haruta, N. Yamada, T. Kobayashi, S. Iijima, J. Catal. 115 (1989) 301.
[3] H.H. Kung, M.C. Kung, C.K. Costello, J. Catal. 216 (2003) 425, and references therein.
[4] Q. Fu, H. Saltsburg, M. Flytzani-Stephanopoulos, Science 301 (2003) 935.
[5] G.C. Bond, D.T. Thompson, Gold Bull. 33 (2000) 41.
[6] J.R. Rostrup-Nielsen, T. Rostrup-Nielsen, CATTECH 6 (2002) 150.
[7] B.C.H. Steele, A. Heinzel, Nature 414 (2001) 345.
[8] W.B. Kim, T. Voitl, G.J. Rodriguez-Rivera, J.A. Dumesic, Science 305 (2004) 1280.
[9] W.B. Kim, T. Voitl, G.J. Rodriguez-Rivera, S.T. Evans, J.A. Dumesic, Angew. Chem. Int. Ed. 44 (2005) 778.
[10] S.K. Desai, M. Neurock, Phys. Rev. B 68 (2003) 075420.
[11] M. Daté, M. Okumura, S. Tsubota, M. Haruta, Angew. Chem. Int. Ed. 43 (2004) 2129.
[12] S. Biella, F. Porta, L. Prati, M. Rossi, Catal. Lett. 90 (2003) 23.
[13] G.M. Brown, M.-R. Noe-Spirlet, W.R. Busing, H.A. Levy, Acta Crystallogr. B 33 (1977) 1038.
[14] P. Gómez-Romero, N. Casañ-Pastor, J. Phys. Chem. 100 (1996) 12448.
[15] S. Kandoi, A.A. Gokhale, L.C. Grabow, J.A. Dumesic, M. Mavrikakis, Catal. Lett. 93 (2004) 93.
[16] T. Bligaard, J.K. Nørskov, S. Dahl, J. Matthiesen, C.H. Christensen, J. Sehested, J. Catal. 224 (2004) 206.